ELSEVIER

Nanomedicine: Nanotechnology, Biology, and Medicine
28 (2020) 102221

nanomedicine
Nanotechnology, Biology, and Medicine

nanomedjournal.com

Temporal sequence of the human RBCs' vesiculation observed in nanoscale with application of AFM and complementary techniques

Magdalena Kaczmarska, PhD[a], Marek Grosicki, PhD[a], Katarzyna Bulat, PhD Eng[a], Mateusz Mardyla, MSc[a,c], Ewa Szczesny-Malysiak, PhD[a], Aneta Blat, MSc[b], Jakub Dybas, PhD[a], Tomasz Sacha, PhD DSc[d], Katarzyna M. Marzec, PhD DSc[a,*]

[a]*Jagiellonian Center for Experimental Therapeutics, Jagiellonian University, Krakow, Poland*
[b]*Faculty of Chemistry, Jagiellonian University, Krakow, Poland*
[c]*Faculty of Motor Rehabilitation, University of Physical Education, Krakow, Poland*
[d]*Chair and Department of Hematology, Jagiellonian University Hospital, Krakow, Poland*

Received 25 October 2019; revised 27 February 2020; accepted 26 April 2020

Abstract

Based on the multimodal characterization of human red blood cells (RBCs), the link between the storage-related sequence of the nanoscale changes in RBC membranes in the relation to their biochemical profile as well as mechanical and functional properties was presented. On the background of the accumulation of RBCs waste products, programmed cell death and impaired rheological properties, progressive alterations in the RBC membranes including changes in their height and diameter as well as the in situ characterization of RBC-derived microparticles (RMPs) on the RBCs surface were presented. The advantage of atomic force microscopy (AFM) in RMPs visualization, even at the very early stage of vesiculation, was shown based on the results revealed by other reference techniques. The nanoscale characterization of RMPs was correlated with a decrease in cholesterol and triglycerides levels in the RBC membranes, proving the link between the lipids leakage from RBCs and the process of vesiculation.

Key words: Red blood cells (RBCs); RBC-derived microparticles (RMPs); Atomic force microscopy (AFM); Packed red blood cells (PRBCs); Membrane alterations

The RBCs are the most common type of blood cells present in the peripheral blood, being well known for their role in oxygen transport.[1] Their function and morphological properties are regulated by the cell membrane, being their principal physical structure.[2] The RBC membrane, which encloses concentrated hemoglobin (Hb) matrix, is strictly connected with the membrane skeleton that maintains the integrity and reversibility of the biconcave disc shape of the RBCs.[3,4] It is important to mention that RBC membranes carry diverse groups of cell surface antigens,[5] either sugars or proteins.[6] The presence of antibodies taking part in adhesion of RBCs to other cells[7] and RBC aggregation related to the antibody–antigen interactions (anti-IgG and IgG antibodies) are commonly studied.[8,9] The other important surface component of RBC membranes is the

Abbreviations: AFM, atomic force microscopy; AS, additive solution ; ATP, adenosine triphosphate; Hb, hemoglobin; LDH, lactate dehydrogenase; MCH, mean corpuscular hemoglobin; MCHC, mean corpuscular hemoglobin concentration; MCV, mean corpuscular volume; PRBC, packed red blood cell; RABs, RBC apoptotic bodies; RBCs, red blood cells; REVs, RBC extracellular vesicles; RMPs, RBC-derived microparticles; SD, standard deviation; SE, standard error

Declaration of interest statement: The authors report no conflict of interests.

This work was supported by the National Centre for Research and Development, Poland (LIDER/13/0076/L-8/16/NCBR/2017).

Author contributions are as follows: M.K.: AFM data collection, analysis, interpretation, drafting the manuscript and design of most figures; M.G., E.S-M.: flow cytometry data collection, analysis and interpretation; K.B.: biochemical data collection and analysis, AFM data collection; M.M.: ektacytometry data collection and analysis; A.B., J.D.: sample preparations for all measurements, hematologic data collection and analysis, design of figures; T.S.: revising the intellectual content and medical expertise; K.M.M.: concept, design, writing and final approval of the version to be published.

Acknowledgment

*Corresponding author at: Jagiellonian Center for Experimental Therapeutics, Jagiellonian University, 30-348 Krakow, Poland. Tel.: +48 12 6645476; fax: +48 12 2974615.

E-mail address: katarzyna.marzec@jcet.eu. (K.M. Marzec).

https://doi.org/10.1016/j.nano.2020.102221

glycocalyx, which is especially important in the context of interaction and adhesion of RBC to other cell types.[7] This extraordinary shape helps RBCs not only to improve the gases exchange efficiency during passage through small capillaries but also to withstand the circulatory shear stress during their 120-day lifespan.[10] Over that time, RBCs must be structurally and mechanically stable to resist fragmentation, which is a common consequence of cell aging. Therefore, cellular deformability is an important determinant of RBCs functionality and survival in the circulation.[11] Moreover, recently it has been proven that the loss of the RBC membrane surface area could be due to the release of the RBCs extracellular vesicles (REVs), structures important for intercellular communication and transport.[12]

Generally, REVs can be divided into three groups. In the previously reported works, REVs' naming and sizes are not accurately defined.[13–16] In this article we will distinguish: RBC exosomes (30-100 nm), RBC-derived microparticles (RMPs; RBC ectosomes, 0.1-1.0 μm) and RBC apoptotic bodies (RAB; 1-5 μm).[17–20] RBC exosomes are formed mainly during RBCs development in the bone marrow and are released by reticulocytes,[21,22] while RMPs and RABs are generated during normal aging of RBCs.[18] There are several hypotheses about the purpose of cellular vesiculation, including maintaining of membrane function and extending the RBCs' life by removing damaged proteins from the mature RBC membrane,[23] cell-to-cell communication with RMPs serving as inter-cellular exchangers of biological material and information[24,25] as well as normal cell development and programmed cell death.[26] REVs are formed in response to various stimuli, such as shear stress, complement attack, proapoptotic stimulation or damage.[27] Their production results in induction of coagulation, immune modulation, ROS scavenging and promotion of endothelial adhesion.[17,18,28] REVs formed in vivo are rapidly scavenged and removed from circulation by Kupffer cells.[29] On the contrary, REVs formed ex vivo inside PCV bags during packed red blood cells (PRBCs) storage accumulate with time and contribute to further RBCs degradation acceleration. This is mainly due to presence of the reactive signaling components inside REVs.[26,30] PRBCs were found to be a reliable source of RMPs for basic and clinical research.[31] However, RMPs obtained from PRBCs represent both RMPs obtained due to the natural process of RBCs aging as well as RMPs produced due to blood processing and storage. RMP composition was found to be affected also by storage conditions.[18] RMPs' formation inside PRBCs might have an important impact on blood transfusion efficiency.[30,32] Therefore, the assessment of the RBCs membrane integrity, biochemical content, and RMPs' presence in the typical PRBCs used for blood transfusion can be used as a valuable marker of RBCs' condition.

As the main triggers of REVs production are the changes in cation gradients, excessive oxidation and metabolic stress, those parameters need to be followed to study the vesiculation processes. During metabolic changes, adenosine triphosphate (ATP) depletion leads to glucose consumption accompanied by an enormous acidosis and 2,3-diphosphoglycerate deprivation, but also significantly impairs the performance of ATP-dependent transporter proteins, such as flippase, floppase and scramblase, three major players responsible for maintaining cell membrane asymmetry.[17,33,34] Energy failure disrupts membrane transporters' activity, leading to an increase in cytosolic calcium and increased potassium leakage.[35,36] These interactions disturb membrane structure by destabilizing its asymmetry and exposing phosphatidylserine (PS), clustering of band 3 protein, decreasing and altering the exposure of CD47 and promoting apoptotic vesicle shedding.[37,38] The loss of cation gradients across the membrane is a consequence of reactive oxygen species activity and oxidative damage, resulting from protein and lipid oxidation.[28,36,37,39,40] This leads to a decrease in the level of reduced glutathione (GSH),[41] a major defense against oxidation. Accumulation of all the above-mentioned injuries to the cytoskeleton and membrane results in an increased vesiculation and extensive membrane loss, which during 120-day lifespan reaches the level of around 20% of RBC membrane area.[42] An effect of all those modifications is connected not only with irreversible changes in RBC morphological shape from smooth biconcave disc, through spiculated echinocytes, to dense spherocytes, but also with the loss of RBC volume regulation and diminished deformability.[37] Damaged and dysfunctional RBCs with PS exposition are removed from the circulation by hepatic Kupffer cells via mononuclear phagocyte system.[18,40]

Each individual RBC is estimated to generate around 230 RMPs during its lifespan.[43] RMPs' structure is defined by cellular MPs model, where the membranes of the MPs are shed from the plasma membrane of stimulated cells, harboring cytoplasmic proteins as well as bioactive lipids implicated in a variety of fundamental processes.[17] According to the general mechanisms proposed for cytoskeleton reorganization leading to RMP formation, promotion of the RMPs takes place through redistribution of the aminophospholipids (phosphatidylserine and phosphatidylethanolamine) from the inner to the outer leaflet of the plasma membrane and occurs selectively in lipid-rich microdomains (lipid rafts/caveolae) within the plasma membrane.[18] Therefore, the RMP membrane is filled with lipid components of the parent cell, such as cholesterol[44] and phospholipids (especially aminophospholipids and sphingophospholipids), and is enriched in the lipid rafts proteins acetylocholinesterase, CD55, flotillins and stomatin.[36] Several aspects, such as the type of the parent cell promoting vesiculation, vesiculation triggering process or storage conditions, determine the type of additional molecules that RMPs can carry: protein band 3, glycophorin A, protein 4.1, synexin, sorcin, immunoglobulins, blood group antigens, as well as Hb and actin — cytoskeletal protein that links Hb with RBC membrane.[17,30,45,46]

The aim of this study was to provide a correlation between the storage-related sequence of the nanoscale changes in RBC membrane in relation to RBC membrane biochemistry, mechanical properties and functionality, throughout 49 days of PRBCs' storage. Data were collected weekly from both cellular fraction of the RBCs and additive solution (AS) used during the PRBCs storage. PRBCs were analyzed with a set of classical techniques such as flow cytometry, ektacytometry, hematologic and biochemical analyses combined with the innovative atomic force microscopy (AFM). This approach enabled us to follow RBC membrane alterations from the first to the last days, with reference to different parameters.

It was previously reported that AFM had been successfully applied for studies of RBCs aging, pathology and inducible alterations, in order to determine their morphology and membrane surface characteristics, namely, nanostructure, nanodefects and membrane mechanical properties such as stiffness,[47–49] elasticity or roughness.[50] The approach to assess the quality of PRBCs with the use of AFM was carried out based on dimension parameters, stiffness measurements,[51,52] analysis of topographic features[53] and cell morphology.[54] AFM was also found useful to measure interaction forces between plasma proteins and antibodies against RBC surface antigen, which has an additional impact on immunohematology field.[55–57] This technique was also applied to measure oligosaccharides[58] and glycocalyx on the surface of the RBCs, the latter in respect to the interactions with endothelial cells.[59]

The technological advance of AFM in visualization of the vesiculation processes in situ on the level of single RBC in nanoscale was presented and linked to the specific loss of lipid fraction of RBCs. A decrease in cholesterol and triglycerides levels in the RBC membrane was correlated to other biochemical, mechanical and functional changes in the RBCs and to the increase of the oxidative stress in the surrounding environment. The studies clearly prove that the lipid fraction release from the RBCs should be linked to the process of RMP production and could be a marker of vesiculation level. Moreover, the significance and utility of AFM in RMP analysis which enables far more detailed and automated analysis, compared to standard methods, are presented.

Methods

Sample preparation

Packed red blood cells (PRBCs, $N = 3$) withdrawn from healthy male donors were purchased from the Regional Centre for Blood Donation and Haemotherapy in Krakow. Informed consent was given by each volunteer before the blood withdrawal and the study conformed with the principles outlined in the World Medical Association (WMA) Declaration of Helsinki as well as Bioethical Commission of Jagiellonian University.

The RBCs in PRBCs were suspended in AS (CPD-SAGM containing citrate, phosphate, dextrose-saline, adenine, glucose, mannitol). Measurements of RBCs aging were carried out for each bag, every 7 days, for 8 weeks. During that time PRBCs were stored at 4-6 °C following WHO recommendations. Studies were performed on the cellular fraction of the RBCs and on the AS obtained by 10-minute centrifugation (500 ×g, at room temperature) according to the scheme presented in Figure 1.

Biochemical analysis

Biochemical tests were performed using an ABX Penta 400 biochemical analyzer (Horiba Medical, Japan). Before the measurements, the necessary calibrations and controls of the analyzed parameters were performed. The analyses were carried out in accordance with the manufacturer's procedures using Horiba reagents. Cholesterol, triglycerides, LDH, glucose, lactate and iron were measured in AS (centrifuged from PRBCs) using colorimetric methods. The total volume of the sample was 300 μl for every donor/bag, each week (last three weeks: 350 μl).

Flow cytometry

PRBCs were analyzed using a standard flow-cytometry method. The multiparametric flow-cytometry acquisition was performed with a BD LSII flow cytometer (Becton Dickinson). Daily instrument quality control was performed to ensure identical operation. For the measurements, cells contained in hermetic blood bags were diluted to 1% in physiological saline solution. For each sample 100,000,000 events were acquired in log mode for forward side scatter (FSC), side scatter (SSC) and fluorescent signals. Data were analyzed using BD FACSDiva Software (Becton Dickinson). Cells contained in hermetic blood bags were stained against PE-conjugated anti-CD47 and FITC-conjugated Annexin V. Both antibodies and other reagents were purchased from BD Biosciences. Additionally, nucleated cells were stained with Hoechst 33342 (Thermofisher). Cellular staining was performed according to the manufacturer's instructions. RBCs were gated according to characteristic log FSC and log SSC parameters as well as low Hoechst 33342 signals.

Atomic force microscopy

The AFM measurements of PRBCs were performed in the air on dried smears, in room temperature with minimized lighting (both natural and artificial). Just before the measurements the smears were produced with used cells fixed with 1% glutaraldehyde (10 min), and stored for 24 h in 4 °C. The measurement of one sample lasted approximately up to 3 h. AFM imaging was performed on WITec confocal CRM alpha 300 Raman microscope combined with an AFM. Non-contact mode (AC) using standard force modulation probes with a nominal spring constant of 2.8 N/m (WITec, Ulm, Germany) was applied. Samples were illuminated through a dry Zeiss objective (EC EPIPLAN 20×/0.4). AFM images of 256 × 256 lines and 512 × 512 lines were collected in air conditions, from three different areas of 25 μm^2, 8 μm^2 and 1.5 μm^2. To determine the diameter and the height of each imaged cell, as well as the changes of RBCs surface and in situ formation of microparticles, cross-sections of the AFM images were analyzed. Statistical significance of the obtained values was tested with one-way ANOVA followed by Tukey's posthoc test (NS, not significant; $*P < 0.05$; $**P < 0.01$, $***P < 0.001$, $****P < 0.0001$, $*****P < 0.00001$).

Approximately 12 images of fixed and dried PRBCs smears from the area of 25 μm^2 were collected weekly from each PRBCs bag ($N = 6$). Such approach allowed us to obtain information from around 10-15 PRBCs per bag per each week. In total, the conclusion about PRBCs height/diameter was delivered from $N = 6$ based on the information obtained from around 60-90 cells per week. Additionally, in order to study the changes of RBCs surface and in situ formation of microparticles in detail, high-resolution AFM measurements were carried out for 3-5 PRBCs per bag per each week. Information on the size of the

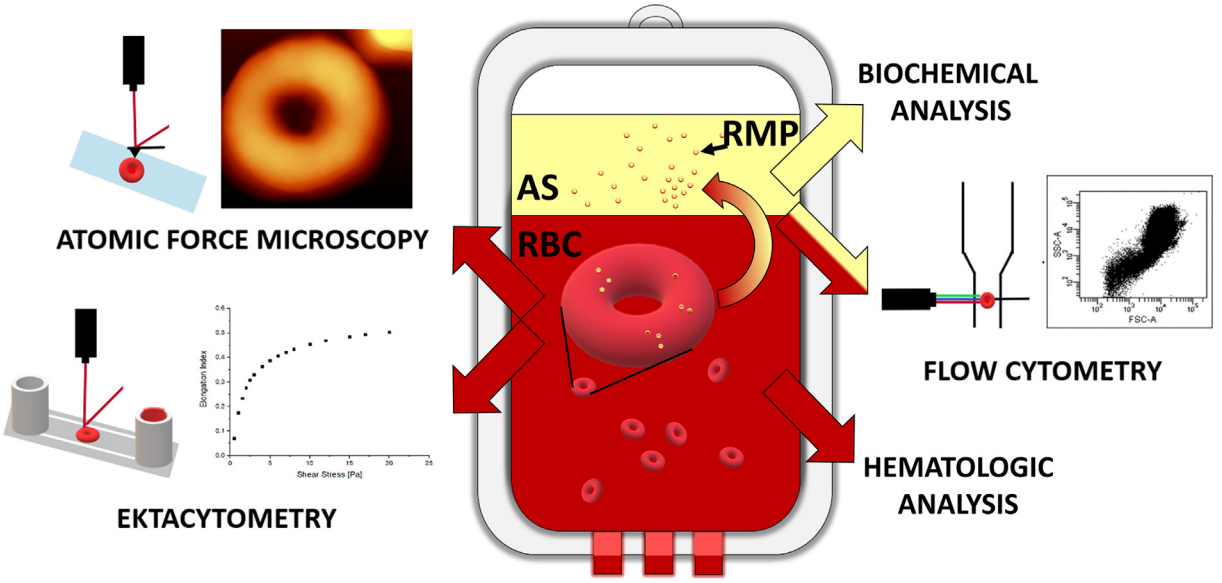

Figure 1. Schematic presentation of the experimental procedure and applied methods, such as biochemical analysis, flow cytometry, hematologic analysis, atomic force microscopy and ektacytometry used to measure changes in the packed red blood cells, respectively, in additive solution (AS), where mainly the RBC-derived microparticles (RMPs) will be released and red blood cells (RBCs) material.

microparticles was obtained from $N = 6$, i.e., around 18-30 cells per week.

To determine the diameter and the height of each imaged cell, cross-sections in two perpendicular planes were made. With use of the principle of the half-height reading from the cellular outline two values of diameter were determined as presented by the profiles marked with numbers 1 and 2 in Figure S6 in SM. Such an approach allowed for minimizing the insensitivity of the scanning cantilever to the *Z*-axis pitch. The height of the cells was estimated based on 4 values, taking into account the ratio of the cell base to the closest prominence, and in this way, the fact that immobilized cells could be lopsided or show morphological changes (i.e. spicules in echinocytes) was taken into consideration, as presented by profiles marked as 1 and 2 in Figure S7.

Hematologic analysis

Morphological parameters including mean corpuscular volume (MCV), mean corpuscular hemoglobin (MCH), and mean corpuscular hemoglobin concentration (MCHC) were determined using a hematology analyzer (ABC Vet, Horiba, Germany). Before each measurement the PRBC samples were mixed. The samples were measured three times according to the manufacturer's instructions.

Ektacytometry

For RBC deformability measurements RheoScanAnD 300 slit-flow ektacytometer was used (RheoMeditech, Seoul, Korea). Hematocrit value was between 55% and 65%. A standard volume of blood (6 µl) was suspended in 600 µl of the isotonic viscous polymer solution, namely, polyvinylpyrrolidine (PVP; RheoMeditech, 360 kDa; pH = 7.4; osmotic pressure: 310 mOsm/kg and viscosity: 30 ± 2 mPa·s). 500 µl of the blood-PVP solution was implemented to one of the plastic disposable reservoirs provided by the manufacturer (RheoMeditech, Seoul, Korea). Fitted results were displayed as a relationship between elongation index (EI) and applied shear stress (between 0.5 and 20.0 Pa). The EI value was calculated with the use of a formula: $EI = (L - W)/(L + W)$, where L is the length and W is the width of the formed diffraction pattern of RBCs flowing through the reservoir's microchannel formed when illumination with 633 nm laser light was applied. All parameters were collected at room temperature (24 °C).

Results

Biochemical analysis

The biochemical analysis of the AS was carried out to define changes in the concentration of chosen parameters taking part in the physiological processes of the RBCs during their 120-day lifespan. We focused on analyzing glucose and lactate levels – the main substrate and product of the RBCs metabolic cycle – as well as lactate dehydrogenase (LDH), which is one of the indicators of RBC membrane destruction and hemolysis that can occur, e.g., during an ongoing oxidative process. The change in free iron concentration in the AS in time corresponds to the level of RBC apoptosis and is proportional to Hb release. Cholesterol and triglyceride concentrations were also studied in the AS to define the level of the lipid-leak from the RBC membrane as the potential indicator of RBC membrane distortion.

As expected, throughout the experiment time frame, high glucose consumption (Figure 2, *A*) was accompanied by an increase in lactate level (Figure 2, *B*). A 50% decrease in glucose concentration during 49 days of RBC storage was detected, starting from a value of ca. 30 mmol/l on the first day and ending with the value of ca. 15 mmol/l. At the same time, the lactate level raised four times, comparing the first (ca. 10 mmol/l) and

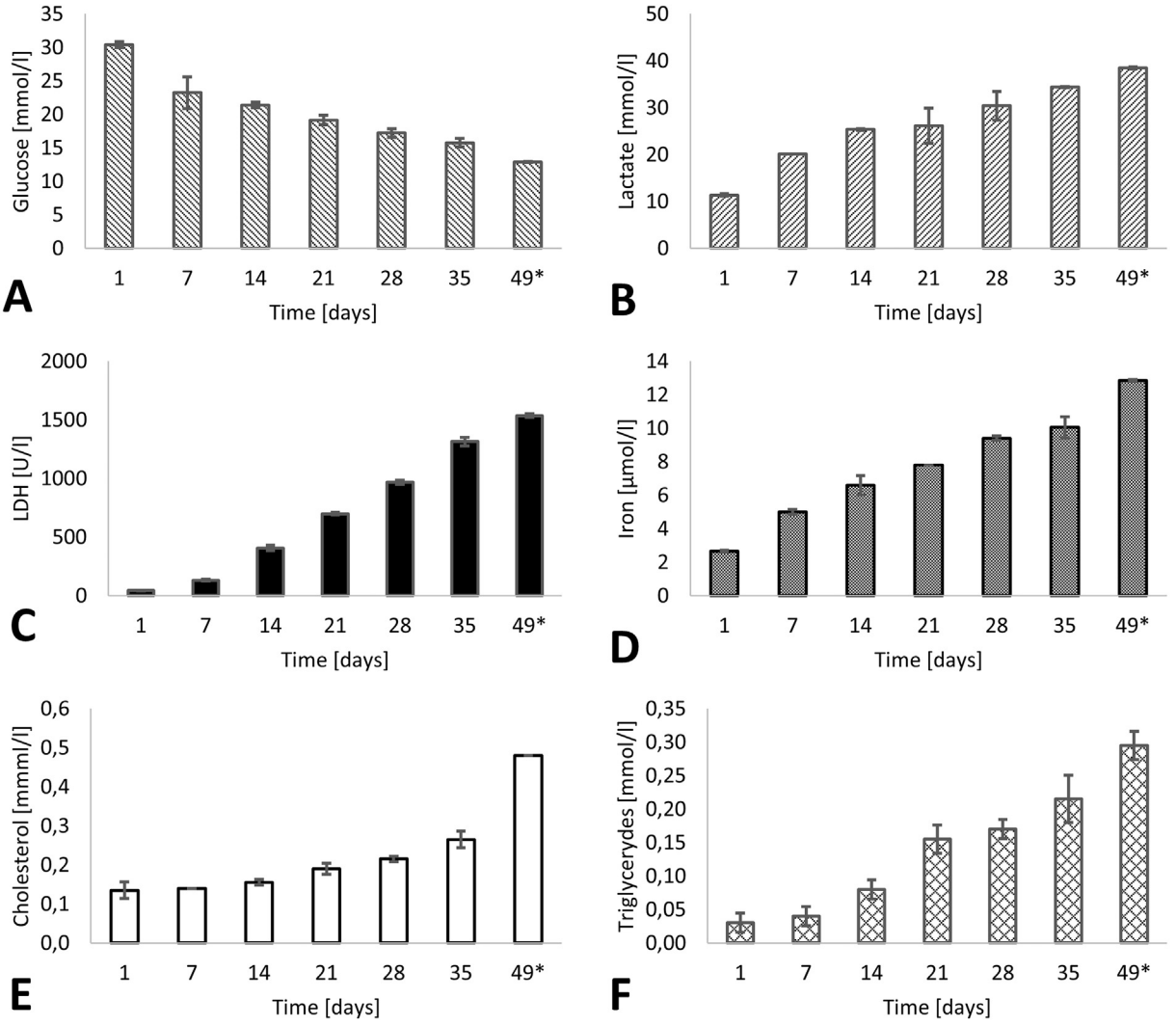

Figure 2. Time-dependent changes in the levels of biochemical parameters: glucose (**A**), lactate (**B**), LDH (**C**), iron (**D**), cholesterol (**E**) and triglycerides (**F**) during the storage of PRBCs.

the last (ca. 40 mmol/l) day of the experiment. These changes indicate the occurrence of severe metabolic stress, which results in energy deficiency and, as a consequence, the formation of ATP during glycolysis.[36,60]

Time-dependent increase in LDH and free iron concentration in the AS was detected (Figure 2, *C*). LDH level was doubled just after the first week of storage and reached the level of ca. 1500 U/l on the 49th day of the experiment (around 40 times higher than on the day one). Similar observations were detected during biochemical analysis of the free iron (Figure 2, *D*). Such an enormous release of LDH enzyme and free iron can point out to the ongoing membrane destruction and RBCs' hemolysis, reflecting an increase in oxidative damage during RBCs' storage what was previously reported and is well documented.[61–65]

Cholesterol and triglyceride measurements showed a 3-fold increase during RBC storage (Figure 2, *E* and *F*) between the first and the last day of the experiment. This observation indicates a disruption of phospholipid asymmetry in the RBC membrane and reduction of its cholesterol[17,18] and triglyceride content.

Flow cytometric analysis

RBCs from the PRBCs were gated according to characteristic $logFSC^{high}/logSSC^{high}$ and Hoechst 33342 $(nuclei)^{negative}$ parameters. Hoechst 33342 $(nuclei)^{positive}$ cells were excluded from the study. Remaining ($logFSC^{low}/logSSC^{low}$) events were defined as cellular debris or RMPs.

Time-dependent increase in the number of apoptotic erythrocytes and a subsequent decrease in CD47 expression level were observed (Figure 3). The number of apoptotic RBC increased from 0.02% of all RBC in the samples on the day 1 of the experiment, up to 0.6% on the day 49th. Simultaneously, a significant (2-fold) decrease in CD47 expression level in the RBC was detected during long-time storage. In contrast, no change in the RBC aggregation (Figure 4) or the number of reticulocytes was detected (Supplementary Figure S13). During the RBC storage, an increase in the number of cellular debris and RMPs was observed (Figure 4). The tendency of changes is quite similar to the observed increase in the triglyceride level in AS

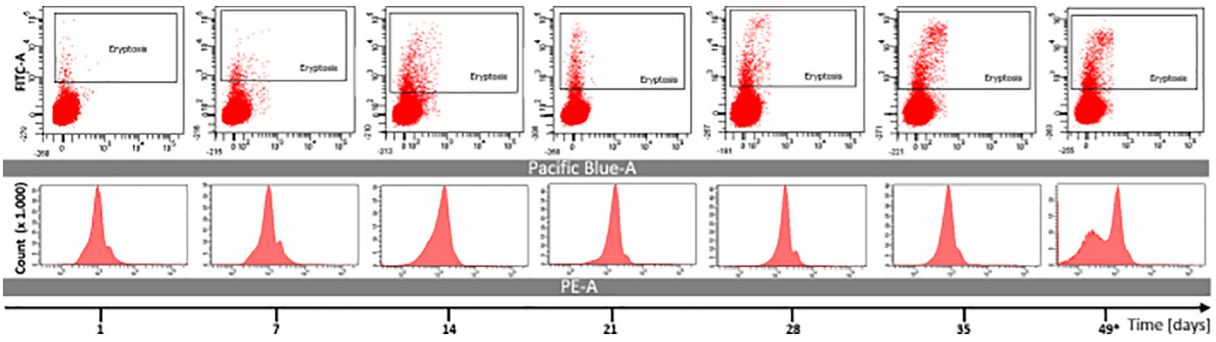

Figure 3. Cytometric analysis of the PRBCs. During the PRBC storage, a time-dependent increase in the number of apoptotic erythrocytes and subsequent decrease in CD47 expression level were observed. RBCs were stained with CD47-PE antibody and FITC conjugated annexin V.

during RBC storage (see Figure 2, *B*). Cellular debris and RMPs (two specific subpopulations) characterized by $logFSC^{low}$/$logSSC^{low}$ parameters, expressed $CD47^{High}$ marker. Over the storage time, increased signals from annexin V were observed, primarily in the REV subpopulation with higher SSC parameter.

AFM imaging and analysis

To observe morphological and structural features of the PRBCs, such as their membrane shape and its nanostructure, the topographical images of the different RBCs' surfaces were recorded using AFM technique.

During the first two weeks (days 1-14) after blood donation, no significant changes in the RBCs' shape or membrane skeleton were observed. RBCs' morphology was characterized by biconcave disc cell shape with a diameter of around 6.0-7.5 μm. High-resolution AFM phase images of the RBC membrane revealed the presence of characteristic RBC skeleton constructed of hexagonal spectrins' network. These observations suggest stability of the PRBC membrane and its proper condition in the second week of PRBC bags storage; however, small protrusions on the RBC surface seen as a kind of blebs of around 130 nm in size[15,66] (marked by white arrows, Figure 5, *B*) were detected (days 1-14). More irregularities in the PRBC morphology were observed in the third week (day 21) of the PRBC bags' storage. As shown in the representative area of the AFM images of 25 μm × 25 μm in size (Figure 5, *A*), other forms than discocytes – spiculed RBCs called the echinocytes –were observed. Moreover, high-resolution AFM images revealed the appearance of membrane structure alterations and formation of the RMPs of a size of around 200 nm or more (Figure 5, *B*), bubbling at the cell surface (marked with arrows). These observations imply that membrane and structure integrity of the RBCs seems to be impaired. The progression of shape changes together with an increase in vesicle formation and grouping of single RMPs in clusters (marked with arrows) on the RBC membrane skeleton was observed during the next two weeks of the PRBCs' storage (days 28-35). The stomatocytes started to appear from the fourth week (day 28), while the spheroechinocytes and spherocytes appeared from 35th to 49th day of storage.

To confirm the progression of the PRBCs' morphological changes observed with the application of AFM technique,[47] a cross-section analysis of each imagined RBC was carried out. Time-dependent changes in the diameter (A) and height to diameter ratio of RBCs (B) detected during each week of PRBCs' storage are presented in Figure 6. The diameter ranges between 4.5 μm, and 8.0 μm. Significant changes in the RBC diameter were noticed between the first two weeks and the last week of storage. On the other hand, the RBCs' height to diameter ratio increased (Figure 6, *B*), which suggests that during PRBC storage the cells become higher and slimmer. Additionally, analysis of the time distribution of erythrocyte shape variability during storage was performed (Figure S8). Such analysis agrees with previous reports and confirms mainly the decrease in the discocytes (20% of the healthy RBCs visible at the beginning of studies decreased to around 5% population at the 49th* day of storage) and an increase of 20% in the echinocytes with the time of storage.[48] Moreover, at the 21st day (in the third week) of PRBC storage, groups of spheroechinocytes and spherocytes (irreversible cells) started to appear, and a concomitant decrease in discocytes was observed.[54]

Such behavior is postulated to be a consequence of the disruption in phospholipid structure of the RBC membrane, and its loss via production of vesicles. These observations are in agreement with the results of the hematologic analysis of mean corpuscular volume (MCV), mean corpuscular hemoglobin (MCH) and mean corpuscular hemoglobin concentration (MCHC) carried out to determine the Hb level and cell volume changes.

Hematologic analysis and ektacytometry measurements

In most cases a slight increase in MCV level (Figure 7, *A*) accompanied by a small decrease in MCHC (Figure 7, *B*) and constant MCH in the SD range (Figure 7, *C*) were observed. These indicate that the RBC area is changing consistently and gradually over time. The functional properties of PRBCs, RBC membrane deformability, and ability to flow via artificial capillary systems were tested using ektacytometry. The analysis showed that the elongation index slowly decreases with PRBC storage time (Figure 7, *D*). Such behavior was previously reported and linked to the disruption in the RBC membrane structure connected with an increase in its stiffness.[67,68] However, contrary to the studied biochemical and mechanical changes, the significant change in their functionality is observed starting from fourth week.

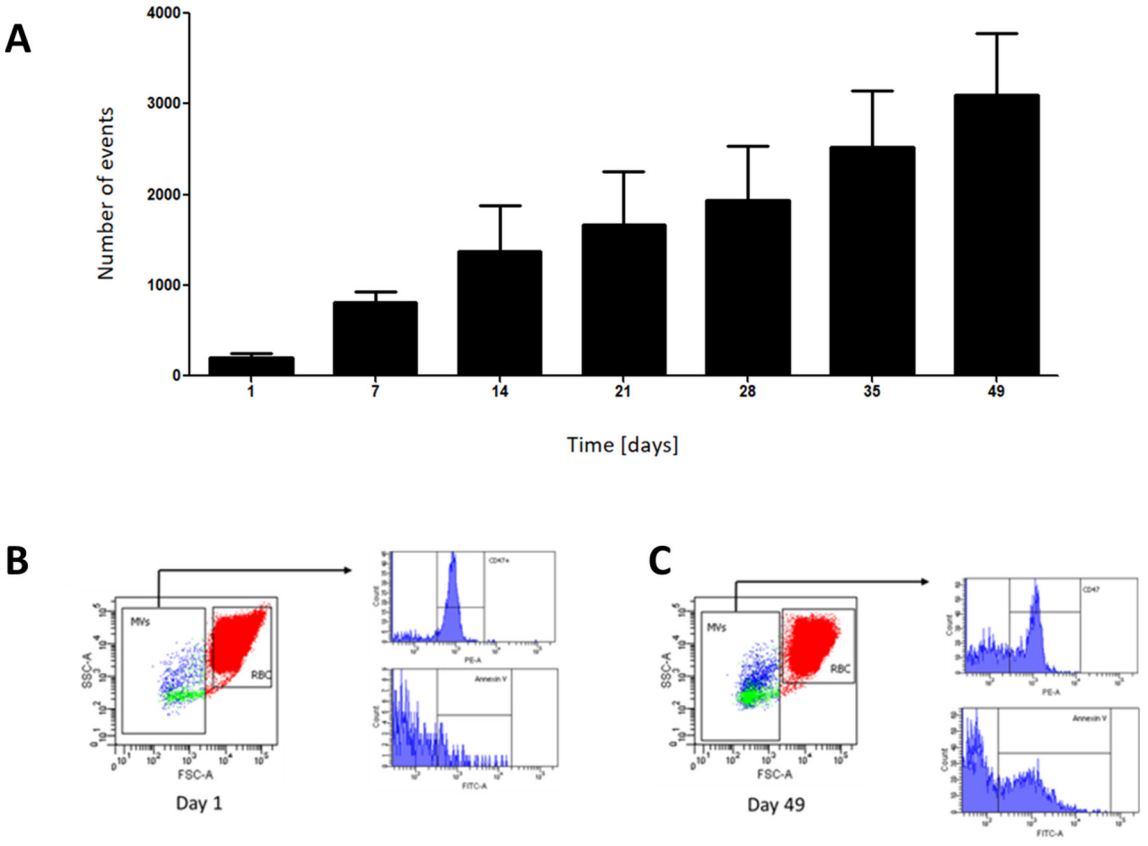

Figure 4. Cellular debris and RMPs. An increase in the number of cellular debris and RMPs were observed upon PRBC storage (**A**). Cellular debris and RMPs characterized by $logFSC^{low}/logSSC^{low}$ parameters, together with $CD47^{High}$ marker (**B**). Over the storage time, increased signals from the annexin V were observed (**C**).

Discussion

The investigation of RMPs' formation, accumulation and pathological effect on RBC physiology is of primary interest of transfusion medicine.[26] RMPs formed in PRBCs during storage, accumulate with time and contribute to irreversible RBC shape and membrane changes.[26] All the structural properties of RBC membrane, including unique protein composition and hexagonal lattice in their membrane skeleton, which maintain RBCs' biconcave disc shape and yet allow for reversible cytoskeleton

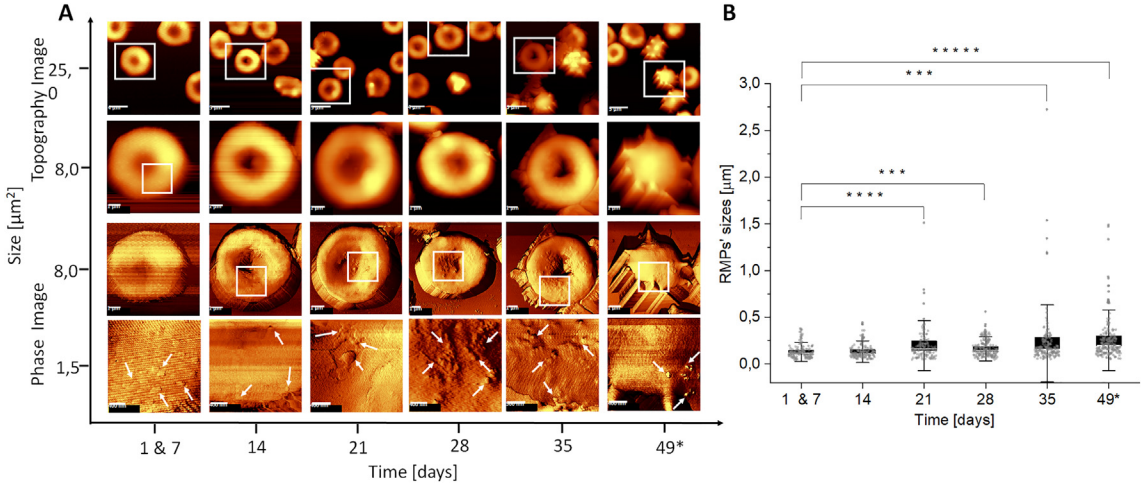

Figure 5. Topography and phase presentations of representative AFM images of the PRBCs' morphological and structural changes in three different scales: 25 μm^2, 8 μm^2 and 1.5 μm^2 (**A**); changes of the RMP sizes observed on the RBCs' surface. (**B**) RMPs' sizes distribution is presented as a box plots (mean value, mean ± SE, whiskers SD). The significance of the differences between the mean values (N=6) was evaluated by one-way ANOVA followed by Tukey's post-hoc test (*P<0.05, **P<0.01, ***P<0.001, ****P<0.0001, *****P<0.00001, ******P<0.0001).

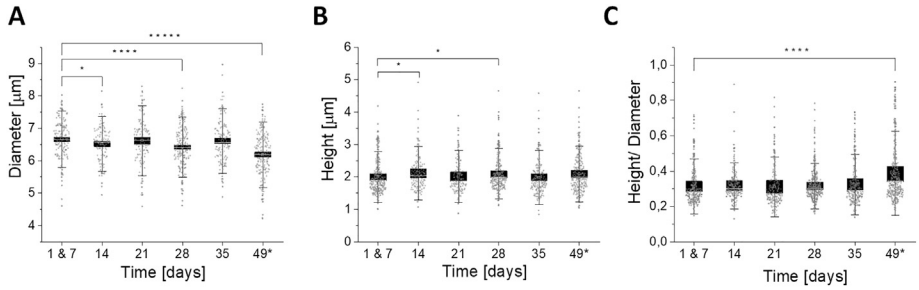

Figure 6. Changes in the diameter (**A**), height (**B**), and height/diameter ratio (**C**) of PRBCs observed on AFM images during storage Data distribution is presented as a box plots (mean value, mean ± SE, whiskers SD). The significance of the differences between the mean values (N=6) was evaluated by one-way ANOVA followed by Tukey's post-hoc test (*P<0.05, **P<0.01, ***P<0.001, ****P<0.0001, *****P<0.00001).

rearrangements during passing through capillaries, could be affected by RMPs' formation and accumulation. In consequence, RBCs altered by RMPs' formation can be characterized by decreased oxygen transport efficiency.[69]

The aim of our study was to investigate storage time-dependent changes in RBC morphology, structure and functionality evoked by formation and accumulation of RMPs using AFM and complementary reference techniques. Our work revealed a specific sequence of the nanoscale changes in RBCs' membrane which was only possible with the AFM-based approach. As presented in Figure 8, the changes on the RBC surface observed with AFM were noticed at a very early stage of vesiculation, even before the occurrence of any detectable biochemical alterations and much earlier than the appearance of functional changes. The disruption in the proper functionality of RBCs' ability to deform (deformability) was confirmed with a gradual decrease of elongation index indicating a dysfunction of the RBC membrane, with significant changes observed starting from the fifth week of PRBC storage. Detectable biochemical alterations were observed from the second week, while the nano-scale membrane alterations were possible to study from the first week of RBC storage.

We visualized in situ production of the RMPs in a single RBC membrane, seen as small protrusions which eventually form RMP clusters on some RBCs. Depending on the storage time, the RMPs had regular shapes and were of around 130 nm in size-[15,66] at the beginning, up to almost 2 µm at the end of the experiment, when the RBCs took the shape of spheroechinocytes with characteristic spicules on the surface. An increase in the RMP size is connected to RMP clustering and appearance of RABs that take sizes >1.0 µm. The first significant increase in their size to approximately 200 nm occurred in the third week of

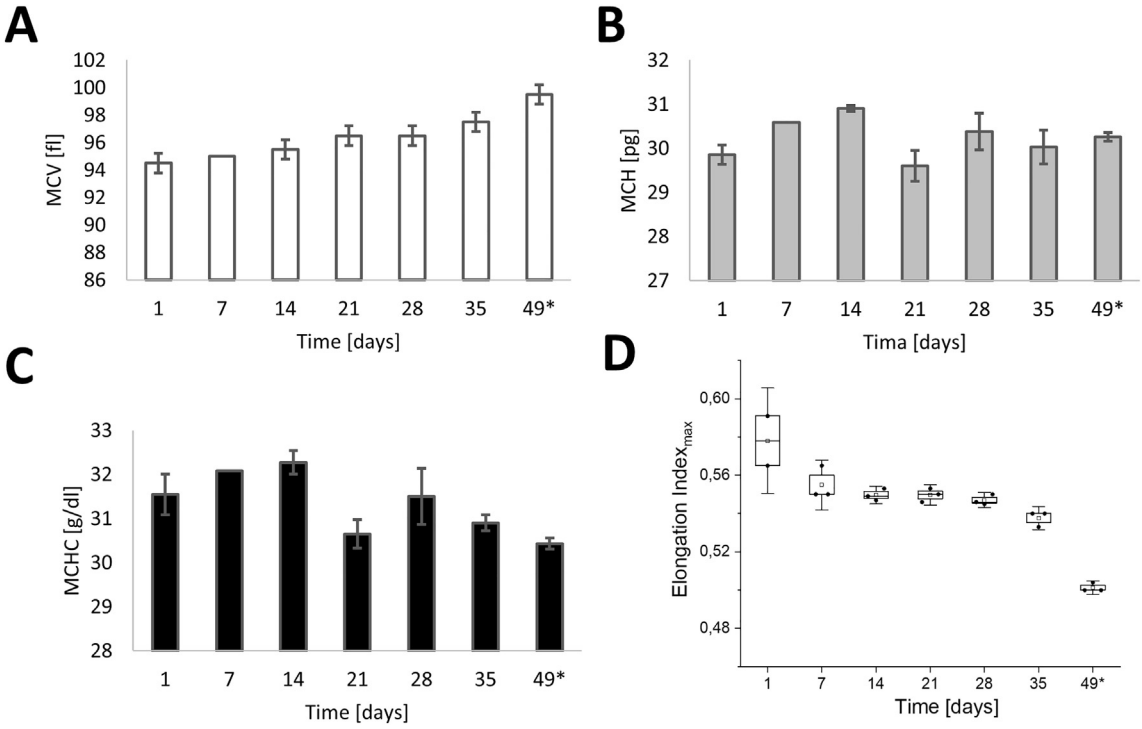

Figure 7. Changes of MCV (**A**), MCH (**B**), MCHC (**C**), EI (**D**) in PRBCs during RBC storage.

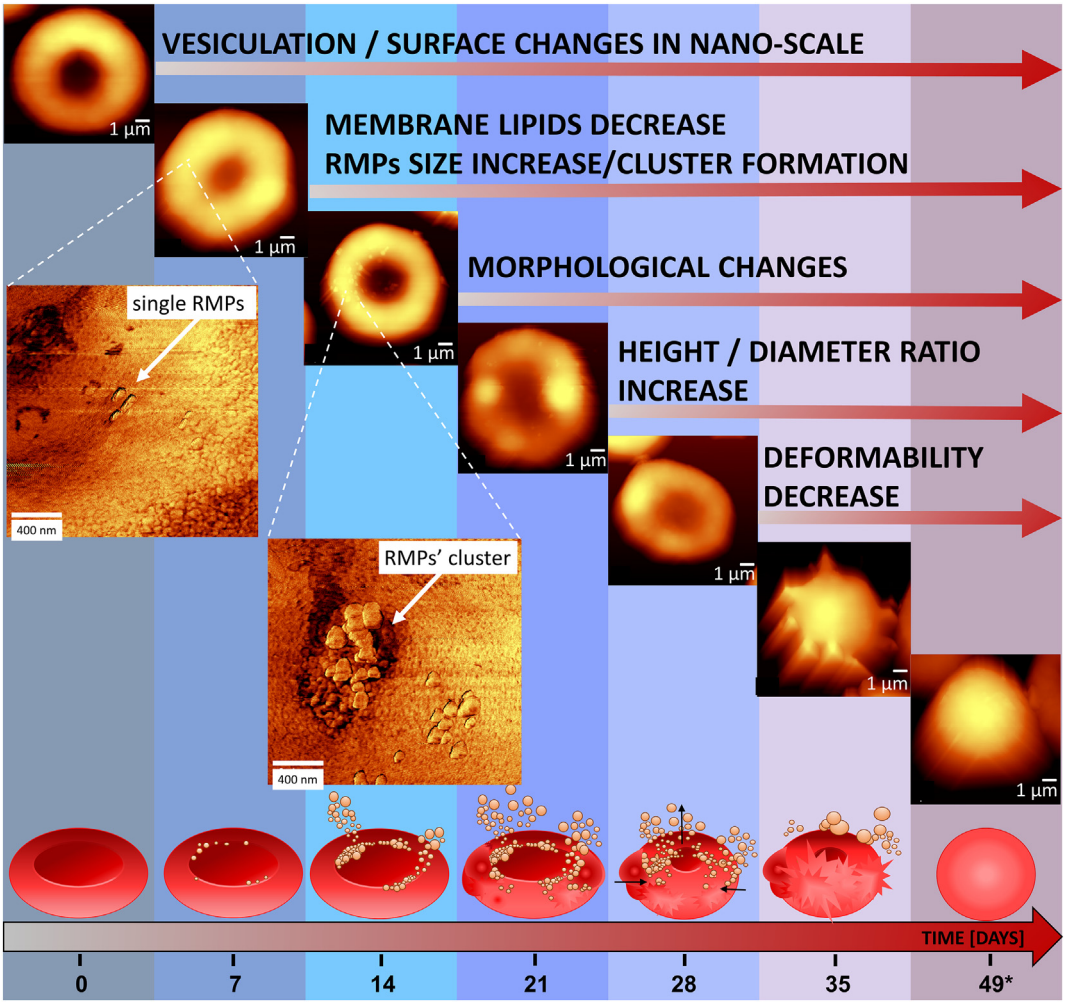

Figure 8. Schematic correlation between storage-related sequence of the nanoscale changes in RBCs' membrane studied with AFM in relation to their biochemical profile as well as mechanical and functional properties.

PRBC storage. After the fifth week, RMP sizes reached even 1500 nm (that is around 20% of a regular RBC size). This is due to either the appearance of RMP clusters or RABs. Additionally, AFM allowed us to visualize the loss of the membrane area which stayed in agreement with the results of biochemical analysis suggesting progressive RBC membrane disruption connected with vesiculation.

We confirmed a gradual increase in the metabolic waste accumulation in the RBCs environment including lactate and free iron levels, along with a decrease in glucose concentration in the AS, from the first days of PRBC storage. This, in turn, triggered RBC membrane alterations that lead to RBCs' vesiculation and, eventually, apoptosis. Flow cytometry results showed that from the second week of storage the expression of CD47 on the outside of the RBC membrane gradually decreased, indicating the disruptions of the RBC membrane connected with ongoing eryptosis and RMP formation.[27,46,70] The level of LDH in the AS increased with time, especially significantly from the second week, suggesting LDH leakage and indicating a further disruption of RBC membrane asymmetry and promotion of vesiculation, which, in consequence, led to a decrease of the RBC area.[61,71] Moreover, we have linked the RMP formation with a decrease of the lipid fraction (from the third week of storage) in RBC membranes, visible as an increase in the lipid fraction in the AS, progressing over time of RBC storage. An increase in cholesterol, as well as triglycerides levels in the AS, came from the lipid content of the RMPs released by the RBCs, and this tendency is also reflected by the numbers of debris observed by flow cytometry. Meanwhile, the RBCs that did not undergo eryptosis swelled to maintain a slight increase in MCV, or at least to keep it on a constant level. This was reflected not only by a steady increase in the RBC distribution width,[23,36] but also by a slight increase in their height, shown for the very first time with the application of AFM. Due to the RBC swelling, the membrane becomes unstable, which, in turn, leads to a breakdown of its asymmetry. In consequence, echinocytes were formed from the third week of PRBC storage, and the further decrease of the RBC membrane area was observed. Current studies suggest that phosphorylation of band 3, a protein important for the structure and morphology of the RBC, disrupts its bond with ankyrin in ankyrin complex, the most important link of the cytoskeleton with the cell membrane. As a result, the RBC transform from biconcave discocytes into echinocytes and the release of RMPs is promoted, which provides another

vesiculation mechanism.[72] This oxidation-driven damage, in consequence, leads to a disruption in the proper functionality of RBCs' ability of reversible shape-shifting.[12,73] As the RBCs do not have membrane renewal mechanisms, ongoing vesiculation causes irreversible damage to the RBC membrane affecting the original RBC morphology and induces a decrease in deformability, which has an impact on the functional properties of RBCs. Such a decrease in functionality expressed as a decrease in RBC deformability, is a result of long-term oxidative stress observed in our studies.

In conclusion, this work demonstrates a specific sequence of the nanoscale changes in RBCs' membrane and correlated it with time-dependent changes in biochemical parameters of PRBCs. Our results prove that stored PRBCs undergo severe metabolic stress and show an increase of apoptosis rate with the time of storage. We have shown that the RMP formation can be correlated with changes of the biochemical profile of the AS, starting from the third week of storage, which is connected mainly with a decrease in the lipid fraction released from RBC membranes. Our work shows that RMPs affect RBC physiology from the very first day of storage, and starting from the first week membrane alterations become noticeable in the nano-scale.

Throughout 49 days with the application of AFM, we have been observing profound changes in RBCs' shape: from smooth biconcave discs in the first two weeks of storage, through echinocytes formed from the third week and spheroechinocytes to rigid spherocytes from the fifth week. These changes were accompanied by REV formation, which varied from 130 nm at the beginning (first week) up to 1500 nm at the end of the experiment (seventh week). Since the first day of RMP storage, the formation and changes in the image of the RBC membrane surface were observed, accompanied by metabolic changes characterized by decreased glucose and increased lactate levels. After 2 weeks of storage, an increase in cholesterol and triglyceride levels was noticed in the AS environment, which is correlated with ongoing vesiculation, which in turn was confirmed by increased cellular debris fraction in flow cytometry analysis. This clearly suggests that the lipid fraction variation in the AS can be linked to the process of RMP production and could serve as a marker of vesiculation level. During the next two weeks morphological changes of the RBCs, namely, the appearance of the cells with changed morphology and sizes, were observed. With the application of AFM technique, we have demonstrated for the very first time that PRBCs change their height and width to maintain an increase in MCV level. The RBCs' deformability changes were noticed, only at the very end of the experiment, on the 35th day of the storage, a week before the expiration date of the PRBC bags.

Our results highlight the usefulness of the application of AFM technique in the combination with biochemical analysis in the studies of the early stage alterations of the RBC membranes correlated with the vesiculation processes. AFM nano-imaging allowed defining the size and shape of single RMPs and their clusters as well as detailed alterations in RBCs' height and diameter. This technique proved to be the most effective in early imaging of RMP production in the nano-scale, being ahead by around one week of the biochemical changes (an increase of lipid fraction in the AS correlated with RMP release) and around five weeks of the functional alterations (a decrease in deformability).

Appendix A. Supplementary data

Supplementary data to this article can be found online at https://doi.org/10.1016/j.nano.2020.102221.

References

1. Ashton N. Physiology of red and white blood cells. *Anaesth Intensive Care Med* 2013;**14**:261-6.
2. De Rosa MC, Alinovi CC, Galtieri A, Scatena R, Giardina B. The plasma membrane of erythrocytes plays a fundamental role in the transport of oxygen, carbon dioxide and nitric oxide and in the maintenance of the reduced state of the heme iron. *Gene* 2007;**398**:162-71.
3. Li H, Lykotrafitis G. Erythrocyte membrane model with explicit description of the lipid bilayer and the spectrin network. *Biophys J* 2014;**107**:642-53.
4. Lux SE. Anatomy of the red cell membrane skeleton: unanswered questions. *Blood* 2016;**127**:187-99.
5. Pourazar A. Red cell antigens: structure and function. *Asian J Transfus Sci* 2007;**1**:24.
6. Dean Laura. Blood group antigens are surface markers on the red blood cell membrane. *Blood groups and red cell antigens*. Bethesda (MD): National Center for Biotechnology Information (US); 2005.
7. Pretini V, Koenen MH, Kaestner L, Fens MHAM, Schifellers RM, Bartels M, et al. Red blood cells: chasing interactions. *Front Physiol* 2019;**10**:945.
8. Yeow N, Tabor RF, Garnier G. Mapping the distribution of specific antibody interaction forces on individual red blood cells. *Sci Rep* 2017;**7**:1-7.
9. Touhami A, Othmane A, Ouerghi O, Ouada HB, Fretigny C, Jaffrezic-Renault N. Red blood cells imaging and antigen-antibody interaction measurement. *Biomol Eng* 2002;**19**:189-93.
10. Kuhn V, Diederich L, Keller T, Kramer CM, Lueckstaedt W, Panknin C, et al. Red blood cell function and dysfunction: redox regulation, nitric oxide metabolism, Anemia. *Antioxid Redox Signal* 2017;**26**:718-42.
11. Badior KE, Casey JR. Molecular mechanism for the red blood cell senescence clock. *IUBMB Life* 2018;**70**:32-40.
12. Huisjes R, Bogdanova A, van Solinge WW, Schiffelers RM, Kaestner L, van Wijk R. Squeezing for life — properties of red blood cell deformability. *Front Physiol* 2018;**9**:656.
13. Danesh A, Inglis HC, Jackman RP, Wu S, Deng X, Muench MO, et al. Exosomes from red blood cell units bind to monocytes and induce proinflammatory cytokines, boosting T-cell responses in vitro. *Blood* 2014;**123**:687-96.
14. Harisa GI, Badran MM, Alanazi FK. Erythrocyte nanovesicles: biogenesis, biological roles and therapeutic approach: erythrocyte nanovesicles. *Saudi Pharm J* 2017;**25**:8-17.
15. Bach Nguyen D, Ly Thi Bich Thuy, Wesseling MC, Hittinger M, Torge, A. Devitt A, et al. Characterization of microvesicles released from human red blood cells. *Cell Physiol Biochem* 2016;**38**:1085-99.
16. Roy S, Hochberg FH, Jones PS. Extracellular vesicles: the growth as diagnostics and therapeutics; a survey. *J Extracell Vesicles* 2018;**7**:1438720.
17. Hugel B, Martínez MC, Kunzelmann C, Freyssinet J-M. Membrane microparticles: two sides of the coin. *Phys Ther* 2005;**20**:22-7.
18. Said AS, Rogers SC, Doctor A. Physiologic impact of circulating RBC microparticles upon blood-vascular interactions. *Front Physiol* 2017;**8**:1120.
19. Gould SJ, Raposo G. As we wait: coping with an imperfect nomenclature for extracellular vesicles. *J Extracell Vesicles* 2013;**2**:20389.

20. Varga Z, Yuana Y, Grootemaat AE, van der Pol E, Gollwitzer C, Krumrey M, et al. Towards traceable size determination of extracellular vesicles. *J Extracell Vesicles* 2014;**3**:23298.
21. Díaz-Varela M, de Menezes-Neto A, Perez-Zsolt D, Gámez-Valero A, Seguí-Barber J, Izquierdo-Useros N, et al. Proteomics study of human cord blood reticulocyte-derived exosomes. *Sci Rep* 2018;**8**:14046.
22. Carayon K, Chaoui K, Ronzier E, Lazar I, Bertrand-Michel J, Roques V, et al. Proteolipidic composition of exosomes changes during reticulocyte maturation. *J Biol Chem* 2011;**286**:34426-39.
23. Bosman G. J. C. G. M., Lasonder, E., Groenen-Döpp, Y. a. M., Willekens, F. L. A. & Werre, J. M. The proteome of erythrocyte-derived microparticles from plasma: new clues for erythrocyte aging and vesiculation. *J. Proteomics* 2012;**76**:203-10.
24. Regev-Rudzki N, Wilson DW, Carvalho TG, Sisquella X, Coleman BM, Rug M, et al. Cell-cell communication between malaria-infected red blood cells via exosome-like vesicles. *Cell* 2013;**153**:1120-33.
25. Xin Zhang, D., Kiomourtzis, T., Kuen Lam, C. & T.N. Le, M. The biology and therapeutic applications of red blood cell extracellular vesicles. in *Erythrocyte* 1-16 (IntechOpen, 2018).
26. Kriebardis AG, Antonelou MH, Stamoulis K, Economou-Petersen E, Margaritis LH, Papassideri IS. RBC-derived vesicles during storage: ultrastructure, protein composition, oxidation, and signaling components. *Transfusion* 2008;**48**:1943-53.
27. Simak J, Gelderman MP. Cell membrane microparticles in blood and blood products: potentially pathogenic agents and diagnostic markers. *Transfus Med Rev* 2006;**20**:1-26.
28. Bodega G, Alique M, Puebla L, Carracedo J, Ramírez RM. Microvesicles: ROS scavengers and ROS producers. *J Extracell Vesicles* 2019;**8**:1626654.
29. Willekens FLA, Werre JM, Kruijt JK, Roerdrinkholder-Stoelwinder B, Groenen-Döpp YAM, van den Bos AG, et al. Liver Kupffer cells rapidly remove red blood cell-derived vesicles from the circulation by scavenger receptors. *Blood* 2005;**105**:2141-5.
30. Greenwalt TJ. The how and why of exocytic vesicles. *Transfusion* 2006;**46**:143-52.
31. W.P. Kuo, J.C. Tigges, V. Toxavidis and I. Ghiran, Red blood cells: a source of extracellular vesicles. in *Methods in molecular biology* (ed. Winston Patrick Kuo, S. J.) vol. 1660 15–22 (2017).
32. Hashemi Tayer A, Amirizadeh N, Ahmadinejad M, Nikougoftar M, Deyhim MR, Zolfaghari S. Procoagulant activity of red blood cell-derived microvesicles during red cell storage. *Transfus Med Hemotherapy* 2019;**46**:224-30.
33. Bevers EM, Comfurius P, Dekkers DW, Zwaal RF. Lipid translocation across the plasma membrane of mammalian cells. *Biochim Biophys Acta - Mol Cell Biol Lipids* 1999;**1439**:317-30.
34. D'Alessandro A, Kriebardis A, Rinalducci S, Antonelou MH, Hansen KC, Papassideri IS, et al. An update on red blood cell storage lesions, as gleaned through biochemistry and omics technologies. *Transfusion* 2015;**55**:205-19.
35. Burger P, Kostova E, Bloem E, Hilarius-Stokman P, Meijer AB, van den Berg TK, et al. Potassium leakage primes stored erythrocytes for phosphatidylserine exposure and shedding of pro-coagulant vesicles. *Br J Haematol* 2013;**160**:377-86.
36. Flatt JF, Bawazir WM, Bruce LJ. The involvement of cation leaks in the storage lesion of red blood cells. *Front Physiol* 2014;**5**:214.
37. Hess JR. Measures of stored red blood cell quality. *Vox Sang* 2014;**107**:1-9.
38. Burger P, Hilarius-Stokman P, de Korte D, van den Berg TK, van Bruggen R. CD47 functions as a molecular switch for erythrocyte phagocytosis. *Blood* 2012;**119**:5512-21.
39. Mohanty JG, Nagababu E, Rifkind JM. Red blood cell oxidative stress impairs oxygen delivery and induces red blood cell aging. *Front Physiol* 2014;**5**:1-6.
40. Lutz HU, Bogdanova A. Mechanisms tagging senescent red blood cells for clearance in healthy humans. *Front Physiol* 2013;**4**:387.
41. D'Alessandro A, D'Amici GM, Vaglio S, Zolla L. Time-course investigation of SAGM-stored leukocyte-filtered red blood cell concentrates: from metabolism to proteomics. *Haematologica* 2012;**97**:107-15.
42. Waugh R, Narla M, Jackson C, Müller TJJ, Suzuki T, Dale GL. Rheologic properties of senescent erythrocytes: loss of surface area and volume with red blood cell age. *Blood* 1992;**79**:1351-8.
43. Bosch FH, Werre JM, Schipper L, Roerdinkholder-Stoelwinder B, Huls T, Willekens FLA, et al. Determinants of red blood cell deformability in relation to cell age. *Eur J Haematol* 1994;**52**:35-41.
44. Orlov D, Karkouti K. The pathophysiology and consequences of red blood cell storage. *Anaesthesia* 2015;**70**:29-e12.
45. Vorselen D, van Dommelen SM, Sorkin R, Piontek MC, Schiller J, Döpp ST, et al. The fluid membrane determines mechanics of erythrocyte extracellular vesicles and is softened in hereditary spherocytosis. *Nat Commun* 2018;**9**:4960.
46. Rubin O, Crettaz D, Canellini G, Tissot J-D, Lion N. Microparticles in stored red blood cells: an approach using flow cytometry and proteomic tools. *Vox Sang* 2008;**95**:288-97.
47. Kozlova E, Chernysh A, Moroz V, Sergunova V, Gudkova O, Manchenko E. Morphology, membrane nanostructure and stiffness for quality assessment of packed red blood cells. *Sci Rep* 2017;**7**:7846.
48. Kozlova E, Chernysh A, Moroz V, Sergunova V, Gudkova O, Kuzovlev A. Nanodefects of membranes cause destruction of packed red blood cells during long-term storage. *Exp Cell Res* 2015;**337**:192-201.
49. Picas L, Rico F, Deforet M, Scheuring S. Structural and mechanical heterogeneity of the erythrocyte membrane reveals hallmarks of membrane stability. *ACS Nano* 2013;**7**:1054-63.
50. Girasole M, Girasole M, Pompeo G, Cricenti A, Longo G, Boumis G, et al. The how, when, and why of the aging signals appearing on the human erythrocyte membrane: an atomic force microscopy study of surface roughness. *Nanomedicine Nanotechnology, Biol Med* 2010;**6**:760-8.
51. Xu Z, Zheng Y, Wang X, Shehata N, Wang C, Sun Y. Stiffness increase of red blood cells during storage. *Microsystems Nanoeng* 2018;**4**:1-6.
52. Lamzin IM, Khayrullin RM. The quality assessment of stored red blood cells probed using atomic-force microscopy. *Anat Res Int* 2014;**2014**:1-5.
53. Santacruz-Gomez K, Silva-Campa E, Álvarez-García S, Mata-Haro V, Soto-Puebla D, P-M M. An AFM approach of RBC micro and nanoscale topographic features during storage biomedical imaging with nanoplatforms for theranostics view project. *Int J Chem Mol Eng* 2014;**8**:410-3.
54. Blasi B, D'Alessandro A, Ramundo N, Zolla L. Red blood cell storage and cell morphology. *Transfus Med* 2012;**22**:90-6.
55. Yeow N, Tabor RF, Garnier G. Atomic force microscopy: from red blood cells to immunohaematology. *Adv Colloid Interface Sci* 2017;**249**:149-62.
56. Allen S, Chen X, Davies J, Davies MC, Dawkes AC, Edwards JC, et al. Detection of antigen-antibody binding events with the atomic force microscope. *Biochemistry* 1997;**36**:7457-63.
57. Dammer U, Hegner M, Anselmetti D, Wagner P, Dreier M, Huber W, et al. Specific antigen/antibody interactions measured by force microscopy. *Biophys J* 1996;**70**:2437-41.
58. Wang H, Hao X, Shan Y, Jiang J, Cai M, Shang X. Preparation of cell membranes for high resolution imaging by AFM. *Ultramicroscopy* 2010;**110**:305-12.
59. Oberleithner H, Wälte M, Kusche-Vihrog K. Sodium renders endothelial cells sticky for red blood cells. *Front Physiol* 2015;**6**:188.
60. van de Watering L. Red cell storage and prognosis. *Vox Sang* 2011;**100**:36-45.
61. Chaudhary R, Katharia R. Oxidative injury as contributory factor for red cells storage lesion during twenty eight days of storage. *Blood Transfus* 2012;**10**:59-62.
62. Verma M, Dahiya K, Malik D, PK S, Devi R, Soni A, et al. Effect of blood storage on complete biochemistry. *J Blood Disord Transfus* 2015;**6**:1-4.
63. Ghezelbash B, Azarkeivan A, Pourfathollah AA, Deyhim M, Hajati E, Goodarzi A. Comparative evaluation of biochemical and hematological parameters of pre-storage leukoreduction during RBC storage. *Int J Hematol stem cell Res* 2018;**12**:35-42.
64. Sanford K, Fisher BJ, Fowler E, Fowler AA, Natarajan R. Attenuation of red blood cell storage lesions with vitamin C. *Antioxidants* 2017;**6**:55.

65. Arif SH, Yadav N, Rehman S, Mehdi G. Study of hemolysis during storage of blood in the blood bank of a tertiary health care centre. *Indian J Hematol Blood Transfus* 2017;**33**:598-602.
66. Almizraq RJ, Seghatchian J, Holovati JL, Acker JP. Extracellular vesicle characteristics in stored red blood cell concentrates are influenced by the method of detection. *Transfus Apher Sci* 2017;**56**:254-60.
67. Burns JM, Yang X, Forouzan O, Sosa JM, Shevkoplyas SS. Artificial microvascular network: a new tool for measuring rheologic properties of stored red blood cells. *Transfusion* 2012;**52**:1010-23.
68. Xu Z, Zheng Y, Wang X, Shehata N, Wang C, Sun Y. Stiffness increase of red blood cells during storage. *Microsystems Nanoeng* 2018;**4**:17103.
69. Mohandas N, Chasis JA. Red blood cell deformability, membrane material properties and shape: regulation by transmembrane, skeletal and cytosolic proteins and lipids. *Semin Hematol* 1993;**30**:171-92.
70. Karon BS, van Buskirk CM, Jaben EA, Hoyer JD, Thomas DD. Temporal sequence of major biochemical events during blood bank storage of packed red blood cells. *Blood Transfus* 2012;**10**:453-61.
71. Rifkind JM, Nagababu E. Hemoglobin redox reactions and red blood cell aging. *Antioxid Redox Signal* 2013;**18**:2274-83.
72. Ferru E, Giger K, Pantaleo A, Campanella E, Grey J, Ritchie K, et al. Regulation of membrane-cytoskeletal interactions by tyrosine phosphorylation of erythrocyte band 3. *Blood* 2011;**117**:5998-6006.
73. Bennett-Guerrero E, Veldman TH, Doctor A, Telen MJ, Ortel TL, Reid TS, et al. Evolution of adverse changes in stored RBCs. *Proc Natl Acad Sci U S A* 2007;**104**:17063-8.